

# Numerical and Experimental Characterization of Wrist-Fingers Communication Link for RFID-based Finger Augmented Devices

S. Amendola, V. Di Cecco, and G. Marrocco

**Abstract**—Radiofrequency-Identification Finger-Augmented Devices (R-FAD) identify a particular wearable technology suitable to turn the human fingers into enhanced sensing surfaces to restore lost senses in impaired people as well as to augment the existing ones. The communication channel of R-FAD, involving a reader's antenna placed onto the wrist and tag antennas stuck onto the fingers, is here characterized in the UHF RFID band by means of both numerical simulations, accounting for several options of the system, and an experimental campaign with volunteers asked to reproduce natural gestures of the hands. The study identifies the most appropriate placement of the devices and, above all, it quantifies the robustness of the link against the human variability. The channel follows a Lognormal Cumulative probability law indicating that the minimum required power to establish a reliable RFID link is 18-27 dBm depending on the chip sensitivity. Measurements finally revealed a remarkable correlation of the minimum required power from the reader with the volume of the hand.

**Index Terms**—Finger Augmented Devices, Flexible Electronics, Radiofrequency Identification, UHF antennas, Wearable sensors, Wireless sensors

## I. INTRODUCTION<sup>1</sup>

Finger Augmented Devices (FADs) are electronic tools, primarily worn on a finger, conceived to modify our interaction with the physical world. Fingers are accordingly considered suitable surfaces for placing electronic components, including small displays and cameras [1], [2], touch-sensitive pads [3], radio-controlled LEDs and vibration motors [4], [5], and even radiofrequency identification (RFID) tags [6], [7]. The ambitious goal of FADs is the achievement of a sensorial *ultrability* according to the two-fold idea of *i*) restoring the natural sensing capability of the hand (for instance the lost or degraded sensitivity to pressure and temperature) and even *ii*) adding completely new senses to capture, for example, the chemical appearance of the things.

An early digital interaction with the things have been investigated for one decade [8], [9], [10]. Wearable radiofrequency scanners were considered in the form of smart gloves and bracelets - mainly working in the HF band - able to detect RFID-signed objects people interact with and, accordingly, to infer the performed activities. From another side, finger-worn

passive antennas, like rings, were more recently investigated at the purpose to establish a radiofrequency interaction with a reader positioned in the external environment [11], [12].

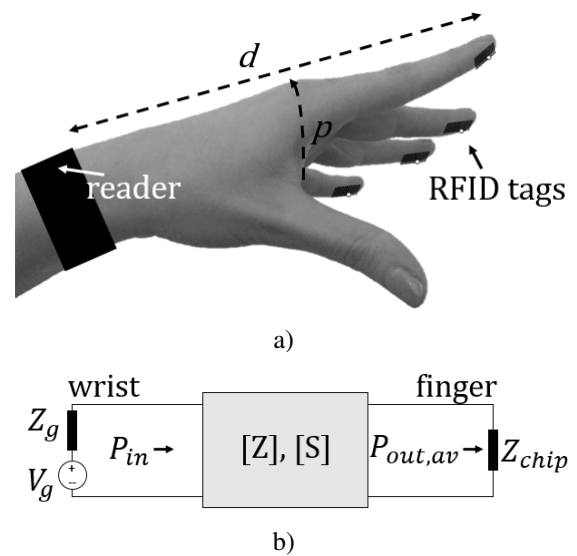


Figure 1. a) Concept of the R-FAD system comprising different finger tags and an interrogating wrist device that is potentially integrable with a smartwatch; b) a two-ports equivalent network.

In a very recent Conference paper, the authors [13] presented a first proof of concept of RFID-based FAD (hereafter R-FAD) having sensing features [7] which merges together the two above architectures as the FAD sensors now interact with a wrist-like reader. The hand-free system comprised an epidermal-like battery-less tag properly shaped around the fingers with sensing capability and an interrogating wristband antenna. This equipment was intended to aid people suffering from Peripheral Neuropathy [14] by artificially restoring the lost temperature feeling of their fingertips as it is aimed to provide the wearer with a real-time feedback about the temperature of the touched objects. However, the reliable application of this system in real life requires to cope with the variability of hands' morphology as well as with the hand gestures performed during the natural interactions with the surrounding objects, which are expected to provoke scattering absorption and shadowing effects.

The wrist-finger RFID setup can be considered as a particular class of wearable system with the specificity of an asymmetric backscattering communication that is typical of

<sup>1</sup>Manuscript submitted on May 22th 2017, revisited on July 20th, 2017, revised on February 25th 2018, further revised on 22th July 2018. Authors are with the Pervasive Electromagnetic Lab at the University of Roma Tor Vergata, Via del Politecnico, 1, 00133, Roma, (ITALY) [www.pervasive.ing.uniroma2.it](http://www.pervasive.ing.uniroma2.it). Corresponding e-mail address: [gaetano.marrocco@uniroma2.it](mailto:gaetano.marrocco@uniroma2.it).

RFID links, as the finger sensor antenna is passive, i.e. it does not include any local power source, and its activation fully relies on energy harvesting.

In the last decades, the huge research efforts on wearable and bodycentric devices have produced a rich set of channel models mostly describing symmetric links for bluetooth and mobile phone applications ([15], [16], [17], [18], [19]). Instead, the few literature concerning RFID links is currently restricted to the out-of the body channel formed by a wearable RFID tag placed onto the clothes [20] or even onto the skin [21] that are interrogated by an external reader, as well as to the transcutaneous links with implanted tags embedded into prosthesis [22], [23]. However, to the best of authors' knowledge, the RFID channel consisting of a wrist reader and finger tags has not yet been addressed. This problem can be considered rather different from those cited above as the interaction between reader and tags occurs in the intermediate distance and, above all, their mutual position is dynamically changed by the natural hand/finger gestures.

Starting from the inception work in [13], this paper provides a detailed investigation of the wrist-finger communication channel for a generic UHF-RFID FAD by analyzing the phenomenology of the electromagnetic interaction and its appropriate numerical modeling up to derive an experimentation-based relationship between the RFID power lower-bound and the size of the hand. Overall, the presented analysis aims at relating the lower-bounds that is required to establish a robust RFID link, to the tags/interrogator arrangements and to different hand gestures accounting also for the user's variability.

The paper is organized as follows. Section II introduces the R-FAD problem, the reference gestures and the wrist and finger antennas while Section III describes the two-port network model and analyzes the phenomenology of the R-FAD coupling. Section IV summarizes the numerical results for the single- and multi-tag configurations, thus identifying the most convenient arrangement. Section V describes an experimental campaign with volunteers to quantify the robustness of the RFID link versus the human variability and to estimate the bandwidth of the reader's antenna required for reliable communication. Finally the R-FAD statistics are discussed in Section VI, where an approximate channel parametrization relating the activation power to the hand form factor is also derived.

## II. THE RFID WRIST-FINGER SYSTEM

The wrist-finger system (Fig. 1.a) includes an interrogation antenna placed over the wrist and connected to a reader unit (to be also mounted on the wrist in the near future) and a conformal tag for application over the fingertip connected to a RFID microchip suitable for sensing. Among the possible options, some sensing-oriented ICs directly provide temperature measurements through an internal solid-state junction (like the EM-4325 or the RFmicron Magnus S3) while more complex ICs are equipped with an internal Analog to Digital Converter and/or an SPI interface (like the AMS-SL900A or

the Farsens Rocky 100) for connecting a dedicated external sensor (for example pressure and humidity). The following investigation will focus on the communication channel, regardless the specific architecture of the IC. This will be only accounted for by IC power sensitivity  $P_{chip}$  (i.e. the minimum RF power required to activate the sensor IC) that is usually better (lower) in case of on-chip sensing functionalities while the use of external sensors usually demand for more power. Establishing a robust RFID link in this arrangement requires to face some numerical and real-life challenges:

i) since a wearable battery-fed reader is needed for a fully embedded wrist-worn device, the available power is rather reduced in comparison with a fixed interrogation station;

ii) both antennas are placed at direct contact with the skin, especially the finger tag; a huge power loss is hence expected to impact on the power requested to activate the tag;

iii) the channel is dynamic as the mutual reader-tag arrangement naturally changes with the hand gestures; accordingly the absorption, shadowing and scattering phenomena are gesture-dependent;

iv) all the electromagnetic interactions occur in the close proximity of the two antennas and moreover in presence of a common supporting medium, such as the arm; accordingly, the channel model deserves a specific investigation;

v) in case of multi-fingers sensors, a further complication may derive from the possible inter-tag coupling.

This Section introduces the reference hand, gestures and the wrist and fingers antennas.

### A. Reference hand and gestures

Let's denote with  $d$  the distance between the wrist and the index finger and with  $p$  the circumference of the palm. The wrist and the finger antennas are preliminarily assumed to be worn (Fig. 2) by a reference homogeneous hand ( $\epsilon_{phantom} = 30$ ,  $\sigma_{phantom} = 0.62$  S/m as in [24]) with  $d=210$  mm and  $p=230$  mm. Since the size of the hand model is rather large, the achieved results can be considered conservative in terms of the required power.

The numerical results presented hereafter were computed by using the transient Finite Integration Technique (FIT) solver of the CST- Microwave Studio 2016 suite which permits to import the CAD models of the hand.

### B. Wrist antenna

The reference wrist antenna (Fig.3) is borrowed from [20]. The layout consists of a shorted patch provided with a miniaturization slot and a partially short-circuit edge that is useful for quick post-fabrication retuning (see the shift of the reflection coefficient in Fig.3). The presence of a ground plane enables a partially electromagnetic decoupling from the arm. The supporting dielectric is a low-permittivity closed-cell PVC foam (Forex) slab ( $\epsilon_F = 1.55$ ,  $\sigma_F = 6 \cdot 10^{-4}$  S/m) able to moderately bend around the wrist. Two possible placements for the patch antenna are i) on the top surface of the wrist (Top-side reader) and ii) on the rear part of wrist (Rear-side reader). For these arrangements of the interrogating patch over

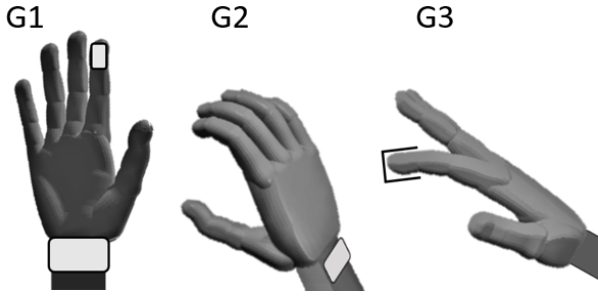


Figure 2. Reference homogeneous hand ( $d=210$  mm and palm perimeter  $p=230$  mm) used for the numerical simulation of wrist-worn patch and finger tags placed in some possible combinations. The three gestures are plane-open (G1), grabbing (G2) and index-touching (G3).

the wrist - whose curvature radius is however rather moderate - a possible bending could occur in the H-plane, i.e making the side  $d$  curved while the side  $a$ , which imposes the resonance, will remain unchanged. Accordingly, as demonstrated in [25], the impact of antenna conformability on the resonance frequency is expected to be negligible.

Under the assumption of 1 W input power (that is typically the highest value allowed by commercial RFID readers), the simulated Specific Absorption Rate (SAR) peak produced inside the hand by the wrist-mounted antenna was SAR=9 mW/kg. This value is much lower than the 2 W/kg limit imposed by the regulation (averaged over 10 grams of tissue) [26]. The RFID-FAD system can be hence considered as fully compliant with the exposure limits.

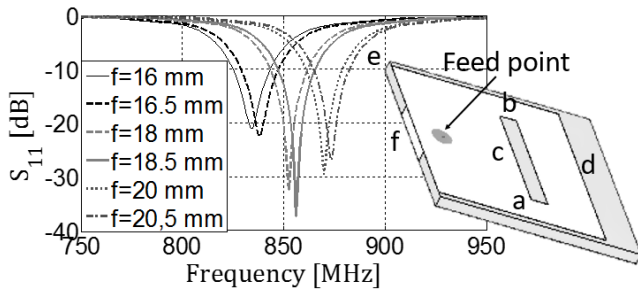


Figure 3. Layout of the wrist-worn folded patch antenna with a tunable short circuit (f). Sizes (in [mm]):  $a=50$ ,  $b=5$ ,  $c=37$ ,  $d=56$ ,  $e=3$ ,  $f=16$ . Example of numerically simulated reflection coefficient of the antenna ( $S_{11}$ ) when placed over the hand model in Fig.2 (gesture G1).

### C. Finger tags

Concerning the finger antennas, we have previously demonstrated in [13] that dipole-like antennas outperform loop-like layout in terms of system power gain. Accordingly, two kinds of Meander-Line-Antenna (MLA) tags are here considered for application over the fingers. The first one is the original layout proposed in [13] comprising a symmetric U-shaped meander-line dipole (hereafter U-tag) suitable to be wrapped around the finger and having the sensitive part, i.e. the microchip, just aligned at the tip of the finger (Fig. 4a). The second configuration is instead a less invasive flat meander-line dipole

(F-tag) to be applied over the distal fingertip thus minimizing bending (Fig. 4b). Without loss of generality, the antennas' impedance are assumed to be matched to a reference<sup>2</sup> common RFID microchip with impedance  $Z_{chip} = 25 + j237 \Omega$  (the simulated power transmission coefficient is reported in Fig. 4.c). Numerical simulations revealed that the power transfer coefficient is slightly sensitive to the particular hand gesture. For example, in the case of the F-tag a frequency shift of  $\pm 10$  MHz was found for the three hand gestures in Fig. 2. Nevertheless, as the bandwidth of the finger antenna is about 30 MHz (referred to  $\tau > 0.75$  corresponding to a read distance not less than the 85% of the peak value), such frequency shift is not expected to produce substantial performance degradations.

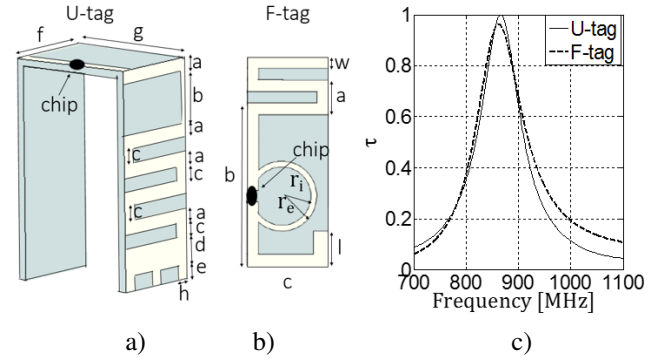


Figure 4. a) Layout of the symmetric Meander-line U-shaped dipole (U-TAG) over a silicone substrate (1 mm thickness) to be used as fingertip tag. Sizes (in [mm]):  $a=1.9$ ,  $b=7.5$ ,  $c=2$ ,  $d=4$ ,  $e=2$ ,  $f=14$ ,  $g=19$ . b) Layout of the Flat meandered dipole (F-TAG). Sizes (in [mm]):  $a=6$ ,  $b=28$ ,  $c=14$ ,  $l=6$ ,  $r=6.02$ ,  $w=a/3$ . c) Example of numerically simulated power transfer coefficient ( $Z_{chip} = 25 + j237 \Omega$ ) of the two tags when placed on the index of the reference hand in Fig.2 (gesture G1).

## III. NUMERICAL MODELS OF WRIST-FINGER COMMUNICATION

In this section, the upper-bound performance of the wrist-fingertip backscattering link is estimated in order to give a measure of the minimum power that is requested to establish a robust RFID communication by considering the reference gestures in Fig.2.

### A. Two-ports model

A general representation of the finger-wrist link, accounting for all the occurring phenomena, can resort to a lossy two-ports network that is characterized through its impedance or scattering matrix (Fig. 1.b). Port 1 and port 2 correspond to the reader's antenna and to the tag terminals, respectively, in the presence of the hand. The recognized metrics [27] to characterize this kind of link is the *Transduction Power Gain* ( $G_T$ ), which is defined as the ratio between the power  $P_{R \rightarrow T}$  delivered by the reader to the chip, in the specific impedance matching condition, and the available power emitted by the reader generator  $P_{av,R}$ :

<sup>2</sup>Additional impedance values will be considered later on.

$$G_T = \frac{P_{R \rightarrow T}}{P_{av,R}} = \frac{4R_{chip}R_G|Z_{21}|^2}{|(Z_{22} + Z_{chip})(Z_{11} + Z_G) - Z_{12}Z_{21}|^2} \quad (1)$$

where  $Z_G$  is the internal impedance of the reader (hereafter assumed as 50 ohm) and  $[Z_{ij}]$  the entries of the impedance matrix of the two-port network. This indicator is useful to compare simulation with measurements, as shown below in Section V. However,  $G_T$  is highly dependent on the specific arrangement of the system (different hand and finger sizes, gestures), so that it is likely to have a possible impedance mismatch at both the reader-antenna port and at the RFID tag-microchip interconnection caused by the dielectric and morphologic variability of the hand. Accordingly the transduction power gain is not suited to provide upper-bound informations, namely the maximum power the reader is able to deliver to the sensor in case of optimal impedance matching (condition chased by the new-generation ICs provided with the self-adjustment impedance capability like the RF-Micron Magnus S3). It is hence more convenient to refer the numerical evaluation of the link budget to an ideal condition implying both the antennas perfectly matched to their impedances for all the considered arrangements. For this purpose the two-port network is parametrized by the *System Power Gain* [28]:

$$g = \frac{P_{R \rightarrow T,av}}{P_{in}} = \frac{|S_{21}|^2}{(1 - |S_{11}|^2)(1 - |S_{22}|^2)} \quad (2)$$

where  $P_{R \rightarrow T,av}$  is the maximum available power that can be delivered to the fingertip antenna's load (in case of a perfect impedance matching),  $P_{in}$  is the power the reader unit delivers to the interrogating antenna and  $[S_{ij}]$  the elements of the Scattering Matrix of the network. The transduction power gain coincides with the system gain in case of perfect impedance matching of both the tag and the reader's antennas.

The wrist-finger communication is well established when the power collected by the fingertip antenna exceeds the IC sensitivity  $P_{chip}$ , i.e. when  $gP_{in} - P_{chip} - p_S \geq 0$ , where all the powers are expressed in dB and  $p_S=3\text{dB}$  is safety margin that, by experience, accounts for the uncertain knowledge of the IC equivalent impedance and sensitivity as well as for the approximate control on the power emitted by the reader.

The minimum input power required to activate the communication in the overall set of the considered gestures in Fig.2 is hence:

$$P_{in,min} = \frac{P_{chip} + p_S}{\min_n \{g_n\}} \quad (3)$$

where  $g_n$  indicates the system gain corresponding to the  $n$ th gesture.

### B. Phenomenology of the R-FAD communication

The presence of the arm in the wrist-finger link, with its high permittivity and losses, is expected to produce a not negligible interaction with the antennas, such as power

absorption, guided waves and scattering. The phenomenology of the electromagnetic interaction is here analyzed by the help of some numerical experiments aimed at understanding the role of the direct path between the two antennas, of the guided waves along the arm and of the power absorption inside the arm itself. For this purpose, the system gain for the reader-tag-arm is evaluated according to five models of increasing approximation (see insets in Fig. 5): *a*) the two-ports network formalism applied to the whole tag-reader-arm (to be considered as reference); *b*) as case *a*) but the hand model has a 2 mm slice cut off the palm to interrupt the dielectric continuity of the arm between the two antennas; *c*) as case *a*) but most of the palm has been removed (7cm slice) from the hand model; *d*) as case *a*) but only the arm and finger portions hosting the two antennas have been preserved. An additional model finally considers *e*) the simple far-field Friis approximation that is usually applied in conventional RFID link budget in the UHF band, and even in case of off-the-body channels. Accordingly, the power  $P_{R \rightarrow T}$  the reader delivers to the tag can be written as  $P_{R \rightarrow T} = P_{in}G_{Reader}G_{Tag}\tau\chi_{RT}\left(\frac{\lambda}{4\pi d}\right)^2$ , where  $\chi_{RT}$  is the polarization loss factor between the reader and the tag and  $G_{Tag}$  and  $G_{Reader}$  are the *embedded* radiation power gains of the tag and reader antennas, respectively, which are independently evaluated in the presence of the arm.  $d$  is finally the distance among the two antennas.

The five tests refer to the G3 gesture, the F-tag and the patch transmitter placed on top the wrist.

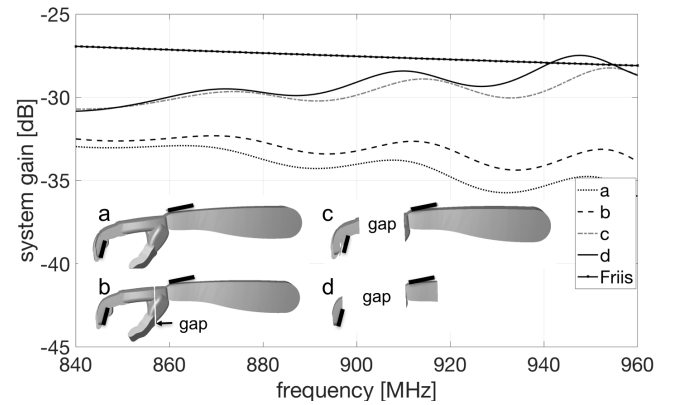


Figure 5. Comparison among the system gains of the wrist-finger system involving the G3 gesture, the F-tag and transmitting patch placed on-top, that are computed according to five different models.

By comparing the profiles of cases *a*) and *b*) it is clear that interrupting the arm does not produce any appreciable change in the system gain and this means that the wrist-finger interaction is not sustained by guided waves (on-body interaction) along the arm while instead it is mostly dominated by radiation. By widening the thickness of the removed slice (case *c*) down to case *d*) the gain increases of 3dB with respect to the un-interrupted structure. This value can be considered as a measure of the power absorption effect of the arm that is more concentrated within the palm, i.e. close to the transmitting patch. Finally, comparison between the

network model of the un-interrupted arm (case *a*) and the approximated Friis model (case *e*) reveals that the far field model, in spite of it already includes the effect of the arm, nevertheless overestimates the system gain of more than 5dB at 868 MHz. Accordingly, the two-port model will be used throughout the following part of the paper to analyze the possible configurations of the R-FAD system.

#### IV. NUMERICAL ESTIMATION OF UPPER-BOUND PERFORMANCE OF THE R-FAD

The minimum power of the reader to activate the tag within various possible options for the wrist and fingers antennas and for the above defined gestures, is here derived by means of numerical simulations considering both single-finger and multi-finger sensor configurations. The following analysis aims at identifying the most effective system arrangement which minimizes the activation power. Such performance indicator has a prominent impact on the power autonomy of the reader.

##### A. Single sensor-tag

For the sake of simplicity, the first configuration refers to a single sensor tag attached on the index finger that is probably the most natural configuration of the hand to touch an object. The minimum power for the interrogating antenna depends on the position of the reader's patch onto the wrist, on the tag layout, and also on the sensitivity of the RFID chip. At this purpose, twelve combinations were analyzed, concerning:

- i) the type of the finger tag (U-Tag, F-Tag);
- ii) the position of the reader's patch (on top-side and rear-side the wrist);
- iii) three hand gestures (plane-open, grabbing, index touching).

For each configuration, the system power gain of the corresponding two-ports network was evaluated from (2).

From Fig.6.a it is apparent that there is a spread of up to 15 dB among the twelve evaluated combinations. The Top-reader/F-tag arrangement is suitable to establish a reliable RFID link with the lowest input power (highest system gain). The minimum input power  $P_{in,min}$  required to activate the communication in all the three gestures can be easily obtained from (3) with the system gain corresponding, case by case, to the three gestures described above. Fig.7 resumes the values of  $P_{in,min}$  for two cases of microchip sensitivity. The first one ( $P_{chip1} = -5 \text{ dBm}$ ) refers to well assessed multi-purpose chips (like the EM Microelectronics EM4325 or the Austrian Microsystem SL900A) suitable to measure the temperature and to drive additional external sensors at the cost of a high power consumption. The second option ( $P_{chip2} = -15 \text{ dBm}$ ) is related to the new generation of identification dies that also provide embedded temperature measurement (like the RFMicron Magnus® S3), even if with a limited configurability when compared with the above chips. By referring to a power limit  $P_{in} \leq 27 \text{ dBm}$  - which is the typical power level of a small-size bluetooth readers - a robust RFID link can be established for all the considered gestures in case of the better sensitivity microchip while the communication success could be borderline for power-hungry ICs.

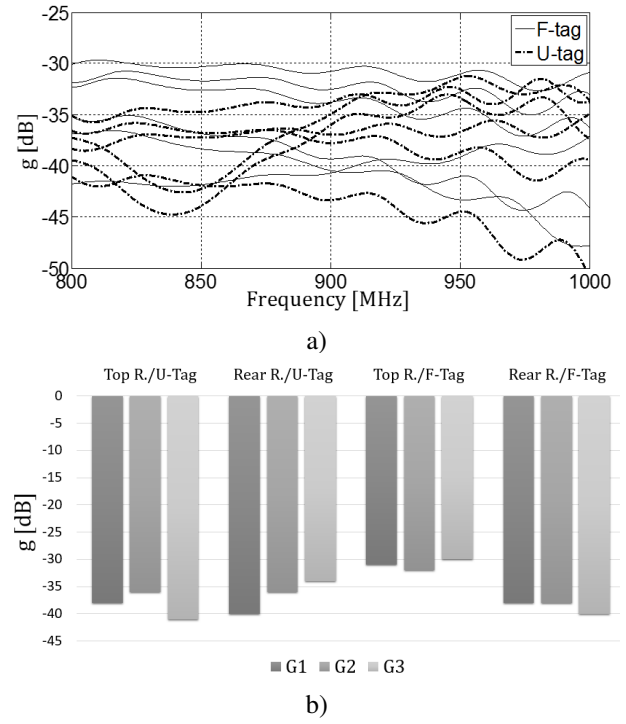


Figure 6. a) Profiles of the numerically-evaluated System Gain of the finger-wrist RFID link for the three gestures of the hand in Fig.2, two types of tag layout and two positions of the reader's antenna on the wrist. b) Comparison at  $f=870 \text{ MHz}$ .

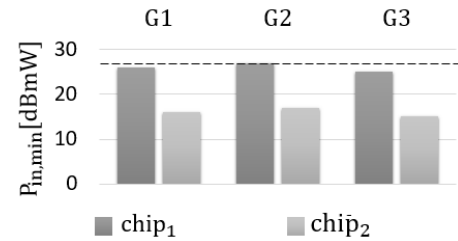


Figure 7. Minimum input power  $P_{in,min}$  through the reader's antenna to activate the RFID link for the case of Top-reader / F-tag configuration for two options of tag sensitivity, in the three hand gestures. The horizontal dashed line at 27 dBm indicates the threshold power level of bluetooth readers suitable to be worn.

##### B. Multi sensor-tags

The more general wrist-finger arrangement comprises five tags, one over each finger, which simultaneously interact with the reader forming a multi-port passive sensor network. For the sake of simplicity only the most effective top reader / F-tag couplet is hereafter considered.

Formally, the five-tags system plus the wrist antenna form a 6x6 interconnected network, already denoted as RFID Grid in [29], with the additional complexity that the reader-tags interaction occurs in the close proximity of a lossy medium. However, the inter-tag coupling is rather modest as numerical simulations revealed that the scattering matrix of the 5x5 network of finger tag is highly diagonal (off-diagonal elements being two order of magnitude lower) due to the



strong absorption effect of the human body that induces an electromagnetic decoupling among fingers. An example of normalized scattering matrix at 868 MHz for gesture G1 is the following:

$$\frac{[|S|]}{\max[|S|]} = \frac{1}{100} \begin{bmatrix} 97 & -0.06 & -0.4 & 0.02 & -0.2 \\ -0.06 & 98 & 0.02 & 0.02 & -0.02 \\ -0.4 & 0.02 & 97 & -0.3 & 0.0015 \\ 0.02 & 0.02 & -0.3 & 97 & 0.3 \\ -0.2 & -0.02 & 0.0015 & 0.3 & 100 \end{bmatrix} \quad (4)$$

Accordingly, the overall system can be simply replaced by five two-port networks (the reader and one tag at a time) to be independently analyzed as in the previous section.

Tab. I resumes the minimum power feeding the reader's antenna at 870 MHz that is sufficient to read the tags over each finger in all the three considered gestures. Overall, the power variation spans within a range of just 5dB thus meaning that the system response looks not heavily influenced by the specific gesture. Under the constrain of maximum reader's power not exceeding 27 dBm, the RFID link could be established in most of the considered configurations. In particular, the requested input power is always much lower than the maximum available value in case of the higher sensitivity chip, while only two configurations among fifteen (IV-G2, V-G1 marked in bold) would be problematic for the case of the lower-sensitivity chip. These results confirm the feasibility of using a low-power reader as a wrist-like device.

Table I

MINIMUM INPUT POWER  $P_{in,min}$  REQUIRED TO ESTABLISH AN RFID LINK WITH TAG PLACED OVER FIRST TO FIFTH FINGERTIP.

	G1		G2		G3	
	$P_{chip1}$	$P_{chip2}$	$P_{chip1}$	$P_{chip2}$	$P_{chip1}$	$P_{chip2}$
I	27	17	24	14	26	16
II	26	16	27	17	25	15
III	25	15	24	14	23	13
IV	27	17	28	18	25	15
V	31	21	27	17	26	16

## V. PROTOTYPES AND MEASUREMENTS

A prototype of the described wrist-finger telemetry system was manufactured to corroborate the above numerical outcomes and to derive some information about the tag response versus the human variability (next Section).

The prototype of the flat meandered fingertip dipole is shown in Fig. 8a. The MLA was fabricated by adhesive copper, carved through a digital controlled plotter, and then stuck over a biocompatible silicone layer (1 mm thickness). The antenna sizes were here optimized over an 80% reduced hand (new size:  $d=168$  mm,  $p=176$  mm) in order to refer to a common average user's hand size (as shown later on in Fig.10 ). The tag was connected to the EM4325 IC (  $Z_{chip} = 23.4 - j145 \Omega$ ,  $P_{chip} = -4.5$  dBm). The tag was tuned in the 850-900 MHz frequency range with a power transfer coefficient  $\tau > 0.5$ .

Finally, silicone handles were glued in the rear side of the antenna to permit a stable placement over the finger as well as an easy repositioning. The patch antenna was soldered to a L-SMA connector and then integrated with a sport wristband for better wearability (Fig. 8b). To measure the RFID link parameters, the patch antenna was connected to a ThingMagic M5e reader having maximum output power of 30 dBm and power resolution of 0.5 dBm.

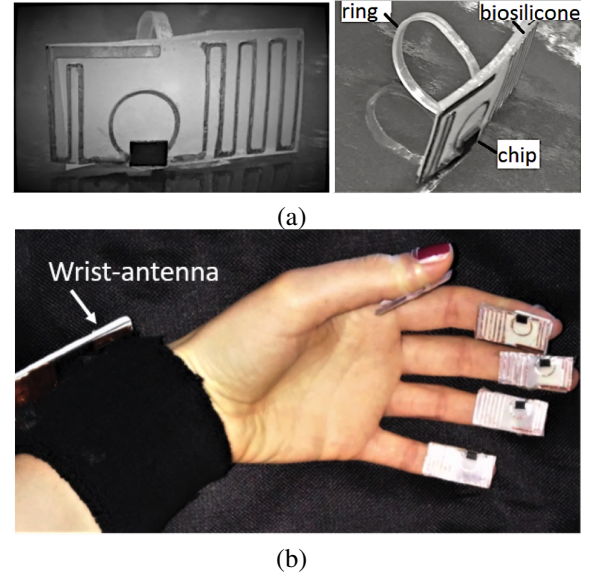


Figure 8. a) Prototype of the fingertip MLA over a bio-silicone substrate (thickness 1 mm). Size (in [mm]), with reference to Fig.4:  $a=1.4$ ,  $b=14$ ,  $c=14$ ,  $d=29$ ,  $l=12$ ,  $r=4.4$ . b) Sensor placement and wrist patch.

The electromagnetic responses of the R-FAD prototype, including all the physical phenomena and in particular the possible impedance mismatching at the two antennas, are here characterized, and then compared with the corresponding simulations, through of the transduction power gain  $G_T$  introduced in Section III.A.  $G_T$  is experimentally derived from the measurement of the turn-on power  $P_{to}$  of the tag. The reader's power is increased until the chip activates and start responding. At the turn-on condition ( $P_{av,R} = P_{to}$ ), the transducer power gain is accordingly determined as:

$$G_T = \frac{P_{chip}}{P_{to}} \quad (5)$$

Fig. 9 shows an example of retrieved transducer power gains corresponding to the five fingers of a volunteer, performing the gesture G1 (open hand), having hand size  $d=175$  mm and  $p=170$  mm, i.e. rather close to that of the simulated reduced model. Similarly to the previous numerical findings (Table I), the responses of the various tags are comparable each other, with a similar peak frequency at  $f_0 \approx 870$  MHz and a span of about  $\pm 3$ dB around the average value. The mean measured data (over the five fingers) and the corresponding simulated outcomes for the scaled hand are comparable apart from a frequency shift of about 20 MHz, probably due to

the manual fabrication tolerances and to the approximation of the electromagnetic parameters of the numerical hand. The 4 dB difference between the peak values has to be ascribed to the simplified homogenous numerical model that overestimates the tissue losses. It is finally worth noting that the larger hand further underestimates the transduction power gain (8dB difference between peaks) because of the larger power dissipation into the hand.

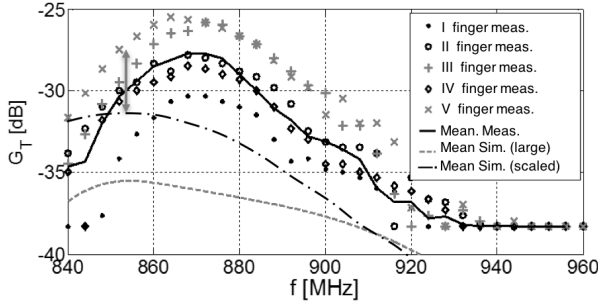


Figure 9. Measured transduction power gain of the wrist-finger RFID link when the sensor-tag is placed over each finger of a volunteer having hand of size  $d=175$  mm and  $p=170$  mm in the gesture G1 and comparison with data from the simulated large ( $d=210$  mm and  $p=230$  mm) and scaled ( $d=168$  mm,  $p=176$  mm) homogeneous hands averaged onto the five fingers.

## VI. EXPERIMENTAL R-FAD LINK CHARACTERIZATION

The R-FAD telemetry system was finally experimented by a set of volunteers at the purpose to extract and parametrize the wrist-finger link behavior.

### A. Test population

The test population comprised ten volunteers (four males and six females) having different size ( $13 \leq d \leq 21$  cm, and  $16 \leq p \leq 22$  cm) of the hands (Fig. 10). The subjects were asked to reproduce the hand gestures in Fig.2 plus other two additional postures as in Fig.11a in order to evaluate a richer set of real-life boundary conditions for the antennas. For the sake of the simplicity, the measurement campaign was limited to the case of a single F-tag placed over the index finger. Overall,  $5 \times 10 = 50$  configurations were analyzed.

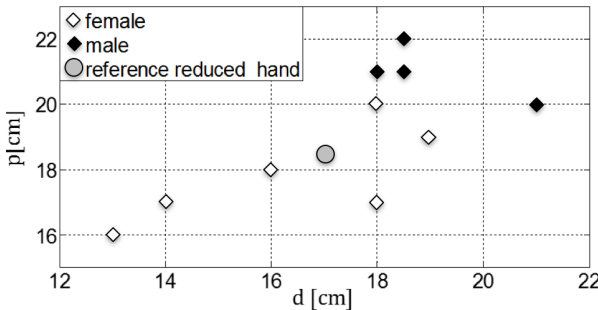


Figure 10. Volunteer's hand size (wrist-finger length and palm perimeters).

### B. Link Statistics

The measurement outcomes concerning the resonant frequency of the tag as well as the transducer power gain have been aggregated at the purpose to provide information about the spread of the RFID link parameters among all the volunteers and all the different gestures. The experimental characterization accounts hence for both the variability of link when a same gesture is repeated by different subjects (inter-subject variability) as well as the variability of the link when the same subject executes different gestures (intra-subject variability)

Fig.11 shows the distribution of the peak frequency of the turn on power. The mean value and the standard deviation are 867.3 MHz and 20.5 MHz, respectively, with a 90% of probability that the peak frequency lays in the 840-890 MHz range. This means that the relative bandwidth of the wrist antenna should be larger than 7% in order to properly trigger the tags in any gestures and for most of the considered volunteers.

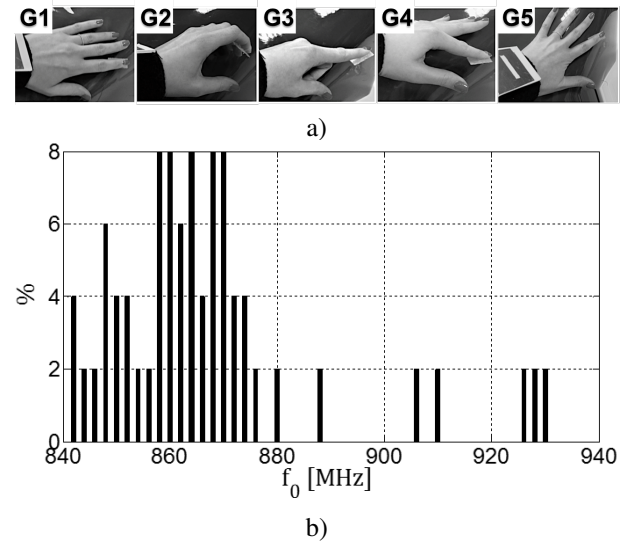


Figure 11. a) Gestures performed by the volunteers: G1: open hand; G2: grabbing; G3: open-hand index touching; G4: close-hand index touching; G5: wide-open. b) Distribution of the resonant frequency of the F-tag when placed onto the index finger of 10 volunteers reproducing the reference gestures .

The measured turn-on powers in case of the microchip sensitivity  $P_{chip,1}$  and the corresponding transduction power gain (as retrieved by inversion of (5)) are resumed in Fig. 12. There is a span of more than 10 dB among the various configurations with an overall average value  $\bar{P}_{to} = 24$  dBm ( $\bar{G}_T = -32$  dB) and standard deviation  $\sigma_P = 3.1$  dBm; the peak of the distribution (25% of the cases) corresponds to a turn-on power  $P_{to} = 26$  dBm ( $G_T = -34$  dB). Fig.13 provides the Cumulative Distribution Function (CDF) of those experiments versus the input power, as estimated for the two considered chip power sensitivities as above. The CDF clearly follows a LogNormal law:

$$\text{LogNormal} = 0.5(1 + \frac{\text{erf}(P_{to} - \bar{P}_{to})}{\sigma_P \sqrt{2}}) \quad (6)$$

where “erf” is the error function. To achieve a 95% of success in the RFID link activation, the reader’s power should be  $P_{in} \geq 27$  dBm and  $P_{in} \geq 17$  dBm in case of the bad and good considered IC sensitivity, respectively. The critical 5% cases occurring during gestures G1 and G2, as found by the numerical analysis.

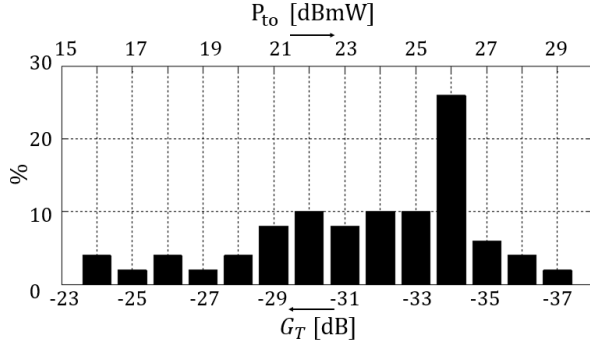


Figure 12. Normalized distribution of transduction power gain at 870 MHz (and of the corresponding turn-on power in case of the microchip sensitivity  $P_{chip,1}=5$  dBm) of the wrist-finger system for all the considered volunteers and hand gestures.

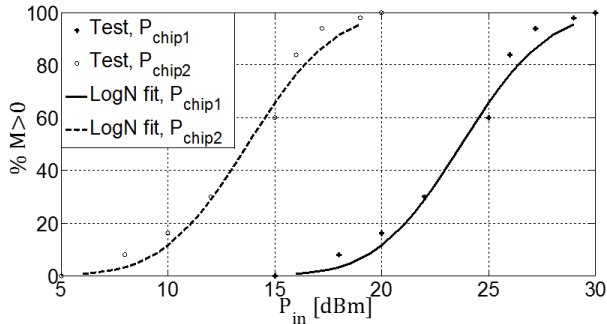


Figure 13. Cumulative Distribution curve of the minimum reader power, for two values of chip sensitivity, and LogNormal fit.

### C. Channel parametrization

The last analysis concerns the possible correlation between the communication performance of the wrist-finger link and the size of the hand. At this purpose, starting from the data in Fig. 12, the transduction power gains were related to three possible parameterizations of the hand, namely the index finger-wrist distance  $d$ , the palm perimeter  $p$  and finally the volume  $V = p^2 d / (4\pi)$  of a cylindrical approximation of the hand. Tab. II shows the corresponding correlation coefficients for each gesture. Overall, there is a slightly better correlation with the hand volume ( $R=0.63$ ), with rather significant values  $R(G_T, V)[G_2]=0.85$ ,  $R(G_T, V)[G_3]=0.81$  for the case G2 and G3 gestures, i.e. the grabbing arrangement and the index-touching that are, perhaps the most common interactions with

objects. This result is in agreement with the phenomenology of the wrist-finger link (see Fig. 5) whose loss mainly occurs in the palm.

The regression approximation (Fig. 14) for these two gestures is:

$$G_T(V)_{dB} = -0.02V - 22.3 \quad (7)$$

and it could be used to arrange a first power budget with a total correlation coefficient of  $R(G_T, V)[G_2 + G_3] = 0.81$ .

Table II  
CORRELATION BETWEEN THE TRANSDUCTION POWER GAIN AND THE SIZE OF THE HANDS.

	G1	G2	G3	G4	G5	all
$R(G_T, d)$	0.27	0.65	0.72	0.54	0.35	0.5
$R(G_T, p)$	0.55	0.77	0.69	0.45	0.35	0.55
$R(G_T, V)$	0.5	0.85	0.81	0.57	0.49	0.63

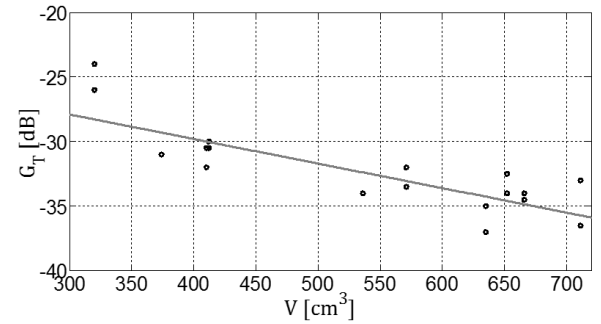


Figure 14. Distribution of the transduction power gains, and regression line, versus the volume of the volunteer’s hand evaluated for the G2 and G3 gestures  $R(G_T, V)[G_2 + G_3] = 0.81$ .

## VII. SUMMARY AND CONCLUSIONS

The paper has derived the communication performance and the power lower bounds of the RFID wrist-finger channel in the UHF band. The main findings are resumed next. *i)* The most effective arrangement for the finger sensor network, among those investigated, involves the reader antenna placed on top the wrist and a compact planar dipole placed onto the distal phalanx. The finger antenna is still open to further improvement especially concerning the skin conformability. At this purpose, the application of the emerging flexible and epidermal electronics could be beneficial. *ii)* Tags over the various fingers have comparable response and, moreover, they are rather mutually decoupled due to the high electromagnetic absorption of the hand. As a consequence, the design of a finger sensor can be referred to the single finger configuration. *iii)* The spread of the resonance frequency observed within the set of volunteers is rather narrow so that a 7% bandwidth reader antenna could be adequate to compensate the tag detuning. *iv)* The overall variation of the transducer power gain and hence of the turn-on power among the various finger is modest: of the order of 5-6 dB, as obtained by both numerical and



experimental tests. Instead, the human variability (hand size and gestures) produces a larger span of 10dB in the required power. v) As most of the power loss occurs in the palm, the reader-tag link gain looks rather correlated to an effective volume of the hand, especially in the case of grabbing and index-touching gestures (the correlation coefficient is  $R > 0.8$ ) vi) Finally, the RFID link follows a Lognormal cumulative probability.

The very conclusive results is that a reader emitting a power of 27 dBm looks suitable to establish the RFID link for the 95% of the considered cases (including person and gesture variations), even for power demanding chips such as the EM 4325 or the AMS-SL900A. Only 18 dBm are instead required by the new generation of sensor-oriented chips which hence allow the use of smaller and longer-lasting reader units.

It is worth stating that the presented analysis only considered, as a first step, the wrist-finger channel as standalone configuration, i.e. without accounting for the presence of the touched object which is likely expected to produce impedance mismatch and, accordingly, a degradation of link performance. The achieved results are certainly meaningful when the finger quickly touches an object and then moves away from it (like the natural gesture to probe very hot surfaces). Accordingly, the link is expected to be degraded, or even interrupted, only for a rather short period and the sensing information could be eventually retrieved immediately after. Nevertheless, a further investigation is needed to explore the behavior of the R-FAD links in the case of a prolonged interaction of the sensorized fingers with surroundings objects and this will be the topic of next papers.

#### ACKNOWLEDGMENT

Work partly funded by Lazio Innova, project SECOND SKIN. Ref. 85-2017-14774.

#### REFERENCES

- [1] C.-H. Su, L. Chan, C.-T. Weng, R.-H. Liang, K.-Y. Cheng, and B.-Y. Chen, "Naildisplay: bringing an always available visual display to fingertips," in *Proceedings of the SIGCHI Conference on Human Factors in Computing Systems*. ACM, 2013, pp. 1461–1464.
- [2] X.-D. Yang, T. Grossman, D. Wigdor, and G. Fitzmaurice, "Magic finger: always-available input through finger instrumentation," in *ACM symposium on User interface software and technology*. ACM, 2012, pp. 147–156.
- [3] H.-L. C. Kao, A. Dementyev, J. A. Paradiso, and C. Schmandt, "Nailo: fingernails as an input surface," in *Conference on Human Factors in Computing Systems*. ACM, 2015, pp. 3015–3018.
- [4] E. Tamaki and K. Iwasaki, "Gesture nail: wireless hand gesture system," *International Journal of Computer Science, Engineering and Applications*, vol. 3, no. 5, p. 29, 2013.
- [5] —, "A half-implant device on fingernails," in *ACM conference on Human factors in computing systems*, 2014, pp. 1447–1452.
- [6] K. C. Vega and H. Fuks, *Beauty Technology: Designing Seamless Interfaces for Wearable Computing*. Springer, 2016.
- [7] R. Shilkrot, J. Huber, J. Steimle, S. Nanayakkara, and P. Maes, "Digital digits: A comprehensive survey of finger augmentation devices," *ACM Computing Surveys (CSUR)*, vol. 48, no. 2, p. 30, 2015.
- [8] E. Berlin, J. Liu, K. Van Laerhoven, and B. Schiele, "Coming to grips with the objects we grasp: detecting interactions with efficient wrist-worn sensors," in *International conference on Tangible, embedded, and embodied interaction*. ACM, 2010, pp. 57–64.
- [9] J. R. Smith, K. P. Fishkin, B. Jiang, A. Mamihev, M. Philipose, A. D. Rea, S. Roy, and K. Sundara-Rajan, "Rfid-based techniques for human-activity detection," *Communications of the ACM*, vol. 48, no. 9, pp. 39–44, 2005.
- [10] K. P. Fishkin, M. Philipose, and A. Rea, "Hands-on rfid: wireless wearables for detecting use of objects," in *Ninth IEEE International Symposium on Wearable Computers (ISWC'05)*, Oct 2005, pp. 38–41.
- [11] W. Farooq, M. Ur-Rehman, Q. H. Abbassi, X. Yang, and K. Qaraqe, "Design of a finger ring antenna for wireless sensor networks," in *European Conference on Antennas and Propagation*, April 2016, pp. 1–4.
- [12] H. Horie and H. Iwasaki, "Wearable finger ring type antenna made of fabric cloth for ban use at uhf and ism bands," in *IEEE MTT-S International*, Dec 2013, pp. 1–3.
- [13] V. Di Cecco, S. Amendola, P. P. Valentini, and G. Marrocco, "Finger-augmented rfid system to restore peripheral thermal feeling," in *IEEE RFID Conference*, 2017, pp. 54–60.
- [14] P. J. Dyck, *Peripheral neuropathy*. Elsevier Inc., 2005.
- [15] B. Zhen, M. Kim, J.-i. Takada, and R. Kohno, "Characterization and modeling of dynamic on-body propagation at 4.5 ghz," *IEEE Antennas and Wireless Propagation Letters*, vol. 8, pp. 1263–1267, 2009.
- [16] T. Aoyagi, M. Kim, J.-i. Takada, K. Hamaguchi, R. Kohno *et al.*, "Body motion and channel response of dynamic body area channel," in *Antennas and Propagation, European Conference on*. IEEE, 2011, pp. 3138–3142.
- [17] R. D'Errico and L. Ouvre, "A statistical model for on-body dynamic channels," *International journal of wireless information networks*, vol. 17, no. 3-4, pp. 92–104, 2010.
- [18] S. L. Cotton and W. G. Scanlon, "Characterization of the on-body channel in an outdoor environment at 2.45 ghz," in *Antennas and Propagation, European Conference on*. IEEE, 2009, pp. 722–725.
- [19] N. Katayama, K. Takizawa, T. Aoyagi, J.-i. Takada, L. Huan-Bang, and R. Kohno, "Channel model on various frequency bands for wearable body area network," *IEICE transactions on communications*, vol. 92, no. 2, pp. 418–424, 2009.
- [20] S. Manzari, C. Occhiuzzi, and G. Marrocco, "Feasibility of body-centric systems using passive textile rfid tags," *Antennas and Propagation Magazine, IEEE*, vol. 54, no. 4, pp. 49–62, Aug 2012.
- [21] S. Amendola, G. Bovesecchi, A. Palombi, P. Coppa, and G. Marrocco, "Design, calibration and experimentation of an epidermal rfid sensor for remote temperature monitoring," *IEEE Sensors Journal*, vol. 16, no. 19, pp. 7250–7257, 2016.
- [22] C. Occhiuzzi, G. Contri, and G. Marrocco, "Design of implanted rfid tags for passive sensing of human body: the stentag," *Antennas and Propagation, IEEE Transactions on*, vol. 60, no. 7, pp. 3146–3154, July 2012.
- [23] R. Lodato, V. Lopresto, R. Pinto, and G. Marrocco, "Numerical and experimental characterization of through-the-body uhf-rfid links for passive tags implanted into human limbs," *IEEE Transactions on Antennas and Propagation*, vol. 62, no. 10, pp. 5298–5306, 2014.
- [24] [Online]. Available: SHO Generic Fore-arm Phantom, <https://www.speag.com/products/em-phantom/phantoms/sho-gfpc-v1/>
- [25] R. R. Ferreira D., Pires P. and C. R.F.S., "Wearable textile antennas: Examining the effect of bending on their performance," *IEEE Antennas Propagat. Magaz.*, vol. 59, no. 3, pp. 54–59, June 2017.
- [26] UE, "1999/519/ce," in *Regulation of the European Union*.
- [27] S. Orfanidis, *Electromagnetic Waves and Antennas*. New Jersey: Rutgers University, August 2010.

- [28] S. Amendola and G. Marrocco, "Optimal performance of epidermal antennas for uhf radiofrequency identification and sensing," *IEEE Transactions on Antennas and Propagation*, vol. PP, no. 99, pp. 1–1, 2016.
- [29] G. Marrocco, "Rfid grids: Part i:electromagnetic theory," *Antennas and Propagation, IEEE Transactions on*, vol. 59, no. 3, pp. 1019 –1026, march 2011.